JOURNAL OF CATALYSIS **122**, 330–345 (1990)

# Activity and Selectivity in Carbon Monoxide Hydrogenation over Rhodium Supported on Pure Zirconia and on K-, P-, and Y-Doped Zirconia

A. BENEDETTI,* A. CARIMATI,† S. MARENGO,† S. MARTINENGO,‡ F. PINNA,* R. TESSARI,* G. STRUKUL,* T. ZERLIA,† AND L. ZANDERIGHI§

**Facoltà di Chimica Industriale, Università di Venezia, 30123 Venice; †Stazione Sperimentale per i Combustibili, Viale A. de Gasperi 3, 20097 San Donato Milanese; and ‡Dipartimento di Chimica Inorganica e Metallorganica and §Dipartimento di Chimica Fisica ed Elettrochimica, Università di Milano, Via G. Venezian 21, 20133 Milan, Italy*

Received December 30, 1988; revised August 7, 1989

Catalysts for the $CO/H_2$ reaction were prepared by supporting $Rh_4(CO)_{12}$ on pure $ZrO_2$, with different phase compositions, and on $ZrO_2$ doped at the surface or in the bulk with $K_2O$, $P_2O_5$, or $Y_2O_3$, and by decomposing the supported carbonyl in a hydrogen stream at 523 or 823 K. The catalysts were characterized by XRD, oxygen and hydrogen chemisorption, TPR, FT-IR/PAS, and catalytic activity measurements both in temperature-programmed experiments and in isothermal condition runs, at atmospheric pressure and with different feed compositions. The phase composition of the support or the doping procedure (bulk or surface) has a minor effect on the physicochemical properties and catalytic activity. Also, the various doping agents, with the exception of $K_2O$, have minor effects. $K_2O$ doping decreases the activity and changes the selectivity of $Rh/ZrO_2$ in the $CO/H_2$ reaction, favoring the formation of oxygenated compounds. Activation at high temperature (823 K) decreases the activity but does not change the selectivity of the catalysts. A significant influence of the feed $H_2/CO$ ratio on activity and selectivity has been found: activity decreases with $H_2/CO$ ratio and selectivity to oxygenates increases. The role of the various parameters investigated is discussed.

## INTRODUCTION

One of the major targets in syngas conversion is the selective formation of higher alcohols, particularly ethanol. Oxide-based catalysts generally promote the selective synthesis of methanol (*1*), while mixtures of higher alcohols (*2*) are obtained by addition of some modifiers. Among the metals, Pt, Pd, and Ir are selective for methanol formation (*3*) under suitable conditions, whereas other group VIII metals, such as Ru, Co, and Fe, are known to be good catalysts for Fischer–Tropsch hydrocarbon formation (*4*), though by modifying the Fischer–Tropsch catalysts it is possible to obtain a certain amount of oxygenated compounds (*5–10*).

Rhodium is a borderline case, because when supported on oxides, it is able to promote the formation of both hydrocarbons and alcohols. Moreover, it has the peculiar property of favoring the formation of ethanol, among the oxygenated products (*11, 12*). It has been suggested that the formation of oxygenated products occurs on oxidized Rh sites, which are able to adsorb carbon monoxide without dissociation (*13–15*), while zerovalent Rh sites dissociate carbon monoxide and are responsible for hydrocarbon formation (*15*).

Both dissociated and undissociated carbon monoxide probably participate in the reactions forming ethanol or higher alcohols, which implies that two different types of active sites might be present on the catalyst. In any case, the type and the nature of the active sites and the reaction mechanism are still a matter of discussion (*16–20*).

Despite the trend to accept the idea of a promoting role of oxidized Rh sites in the formation of methanol, it is not yet clear

0021-9517/90 $3.00

how these sites can be produced and stabilized. The chemical and the physical nature of the support, the dispersion of rhodium, and the morphology of its particles on the support must have a certain role. It has been observed that $SiO_2$ and $Al_2O_3$ (*11*) increase the selectivity to hydrocarbons; ZnO, MgO, and CaO to methanol; and $ZrO_2$, $TiO_2$, and $La_2O_3$ to ethanol (*21*). Tentatively, as a general consideration, one may say that supported rhodium promotes the formation of hydrocarbons on acidic oxides, the formation of methanol on basic oxides, and the formation of ethanol and higher alcohols on amphoteric oxide supports.

According to some authors, the support may not only change the electron density of highly dispersed rhodium, and therefore its reactivity, but may itself be involved in the catalytic process through its acidic and basic sites (*22, 23*). For instance, it has been suggested that CO chemisorbed in proximity to the borderline between the rhodium particles and the support can give either a bridged species, by interaction of the oxygen atom with a coordinatively unsaturated metal atom of the support (*23*), or a formate-like species, by interaction of the carbon atom with an oxygen atom of the support (*15, 24*). The behavior of the support has also been discussed in terms of oxophilic and basic properties (*20*).

Another important aspect is the mobility of support surface layers with consequent migration and possible "covering" of the rhodium particles (*25*). This phenomenon seems to be the main cause of the so-called strong metal–support interactions (SMSI) (*26*) and strong metal–promoter interactions (SMPI) (*27*) evidenced by the decrease in hydrogen chemisorption on catalysts pretreated at high temperature.

In this paper we report a study of the effect of the support on the activity and selectivity of rhodium in the CO hydrogenation reaction. For this purpose zirconium oxides have been prepared with different phase compositions, or doped, both in the surface and in the bulk, with oxides having either a basic ($K_2O$) or an acidic ($P_2O_5$) character or "oxophilic" properties ($Y_2O_3$).

## EXPERIMENTAL

*Support preparation.* $ZrO_2$ was prepared from $ZrOCl_2$ (Hoechst) dissolved in distilled water. By adding a solution of ammonia (20% v/v), a gel of zirconium hydroxide was obtained, which after filtration was washed several times with diluted ammonia solution (pH 8, $T = 323$ K) until no chloride ions were observed in the washings. The hydroxide was then heated at 383 K for 12 h and divided into two parts.

The first part was heated with dry air in a fluidized bed, from room temperature to 823 K at the rate of 3 K/min and then held at this temperature for 2 h.

The second part was heated in an oven using the same procedure but under vacuum (1.33 Pa). Hereafter this support is indicated by the letter "V" (vacuum).

Supports doped with potassium, yttrium, or phosphorus with an atomic ratio Zr/doping component equal to 100 (0.31% w/w for K, 0.71% for Y, and 0.25% for P) were prepared by two procedures:

1. Surface doping: The incipient wetness impregnation technique was used. One-tenth molar solutions of KOH, $Y(NO_3)_3$, and $H_3PO_4$ were added dropwise onto degassed $ZrO_2$ previously calcined at 823 K. The sample was allowed to equilibrate overnight, heated at 383 K for 15 h, and then calcined in a fluidized bed for 2 h at 823 K. These supports are referred to as $ZrO_2/K$, $ZrO_2/Y$, and $ZrO_2/P$.

2. Bulk doping: Freshly prepared zirconium hydroxide was suspended in water and a 0.1 *M* solution of the doping agent was added dropwise with stirring. The mixture was stirred overnight, heated at 383 K for 15 h, and finally calcined as previously described. Hereafter these supports are indicated by the letter "B".

*Catalyst preparation.* The support was heated at 823 K in dry air overnight, cooled under $N_2$ to room temperature, and then transferred into a flask containing anhydrous pentane under $N_2$. A $Rh_4(CO)_{12}$ pentane solution was added dropwise to the suspension under stirring. During this operation the added metal carbonyl solution turned colorless, indicating adsorption of the carbonyl onto the support. When the addition was complete, the stirring was stopped, the colorless solvent was decanted, and the solid was dried under vacuum (1.33 Pa) at room temperature for 1 h; a light brown catalyst powder remained.

The amount of $Rh_4(CO)_{12}$ used corresponds to 1% Rh (w/w) on $ZrO_2$; preliminary tests showed that the solvent remains uncolored until 1.3–1.5% Rh (w/w) is deposited on the support. All catalysts were stored under nitrogen.

*Characterization.* The surface area of the supports was determined by the BET method. Dispersion of the supported rhodium was measured by oxygen and hydrogen chemisorption and by $O_2$–$H_2$ titration, using a pulse flow technique. Thermal treatments, prior to chemisorption measurements, involved heating under 5% hydrogen in argon (40 ml/min) from room temperature to the chosen activation temperature [low-temperature reduction (LTR) at 523 K or high-temperature reduction (HTR) at 823 K] at 10 K/min and holding at that temperature for 2 h under pure hydrogen and then in an argon stream at the same temperature for 3 h. The samples were finally cooled to room temperature in an argon flow. $O_2$ and $H_2$ chemisorption measurements were carried out at 298 K, while the titration of $O_2$ chemisorbed at 298 K was performed with $H_2$ at 373 K.

Fourier transform infrared photoacoustic (FT-IR/PA) spectra of pure carbonyls and freshly prepared catalysts were obtained with a Nicolet 6000C spectrometer equipped with a PAR photoacoustic cell (KBr window) at 8 $cm^{-1}$ resolution and a mirror speed of 0.176 cm $s^{-1}$. Carbon black was used as a reference. The samples (about 25 mg) were transferred into the sample cell carrier in a glove box under nitrogen atmosphere and then flushed with helium for 1 min.

XRD patterns were collected on a Philips vertical goniometer using a highly stabilized X-ray generator (Ni-filtered Cu$K\alpha$ radiation); a proportional counter and a step-by-step technique were employed (steps of 0.02° and $2 \times 10^4$ pulses per angular abscissa).

Temperature-programmed reduction (TPR) measurements were carried out in a stainless-steel tubular reactor equipped with a forced ventilation oven, PID temperature programmer, mass flowmeters, automatic sampling valves, and a HP-5890 gas chromatograph. Freshly prepared catalyst (1 g) was loaded into the reactor under helium flow, hydrogen was then fed at 1200 GHSV, and the temperature was raised from 298 to 523 K at the rate of 2 K/min while the outlet gas was sampled automatically and analyzed by gas chromatography. After cooling to room temperature in helium the reactor was fed with CO for 1 h and the TPR run was repeated. This equipment was also used to perform temperature-programmed reactions in a $H_2$–CO flowing mixture from room temperature to 523 K.

*Catalytic activity.* The activity and selectivity of the catalysts were studied at atmospheric pressure in a Pyrex tubular reactor, operated under differential conditions, heated in a fluidized sand bath with an external oven. The temperature was controlled by a thermocouple inserted into the catalyst bed. The catalyst was diluted in a 1 : 5 ratio with carborundum (60–100 mesh) to minimize temperature gradients. The freshly prepared catalyst (1.2 g) was heated in a hydrogen stream (40 ml/min) at either 523 or 823 K for 2 h before cooling to the reaction temperature. The reaction conditions were temperature 493 K, total pressure 0.101 MPa, $H_2 : CO = 3 : 1$, and GHSV = 1000. Reactants and products were analyzed by gas chromatography using thermal conductivity and flame ionization detectors. Calibration curves of the individual components of the reaction mixture were used for quantitative analysis.

## RESULTS

### *Support Characterization*

XRD analysis of the $ZrO_2$ samples showed the presence of peaks corresponding to the tetragonal (t) and monoclinic (m) phases. Owing to the high percentage of the monoclinic phase, it was not easy to distinguish between cubic and tetragonal phases. To prove the presence of the tetragonal phase some samples, taken from the same amorphous $Zr(OH)_4$ gel, were calcined at a lower temperature, thereby giving a lower content of the monoclinic phase (*28*). In this way the doublet given by the 004 and 400 reflections of the tetragonal form, in the range 69.5–77.5°, was clearly detectable.

To determine the amount of crystalline monoclinic phase in the supports, a procedure of pattern decomposition by best-fitting the peak profile, according to an already established method (*29*), was used to overcome the noticeable overlap of X-ray reflections. The volume fraction of the monoclinic phase [derived from the integral intensity of the three reflections 111, 111(m) and 111(t)] was calculated by applying a known procedure (*30*).

XRD analysis data are reported in Table 1 together with the corresponding BET surface areas. All supports show similar surface areas and phase compositions, with the exception of $ZrO_2$(V) for which the phase composition becomes similar to those for the other supports (tetragonal/monoclinic = 13/87), when heated in air at 823 K for 2 h.

TABLE 1

BET Surface Area and Phase Composition of the Supports

| Support | Surface area ($m^2/g$) | Phase composition (t/m)[a] |
|---|---|---|
| $ZrO_2$ | 93 | 13/87 |
| $ZrO_2$(V) | 118 | 52/48 |
| $ZrO_2$/K | 90 | 12/88 |
| $ZrO_2$/Y | 98 | 15/85 |
| $ZrO_2$/P | 92 | 13/87 |

[a] t, tetragonal; m, monoclinic.

TABLE 2

Rh Dispersion after Hydrogen Activation at 523 K[a]

| Catalyst | D | | |
|---|---|---|---|
| | $O_2$ | $H_2$ | $O_2/H_2$[b] |
| Rh/$ZrO_2$ | 76 | 59 | 65 |
| Rh/$ZrO_2$-V | 79 | 72 | 74 |
| Rh/$ZrO_2$/K | 89 | 87 | 87 |
| Rh/$ZrO_2$/K(B) | 71 | 67 | 70 |
| Rh/$ZrO_2$/Y | 90 | 75 | 81 |
| Rh/$ZrO_2$/Y(B) | 89 | 75 | 78 |
| Rh/$ZrO_2$/P | 93 | 64 | 79 |
| Rh/$ZrO_2$/P(B) | 90 | 65 | 80 |

[a] Stoichiometries assumed: $Rh_2O_3$ and Rh–H.

[b] ml (STP)/g Rh of $H_2$ consumed at 373 K after titration of $O_2$ chemisorbed at 298 K.

### *Hydrogen and Oxygen Chemisorption*

Chemisorption data and the corresponding metal dispersion for the catalysts heated at 523 K in hydrogen flow (LTR) are summarized in Table 2. The results indicate a high dispersion of rhodium, with a mean particle size between 1.5 and 2.5 nm. No significant differences between surface- and bulk-doped catalysts are evident, except for the K-doped ones. The dispersion values obtained from oxygen chemisorption are always greater than those from hydrogen chemisorption, while the values from $O_2/H_2$ titration are in between. Also in this respect, K-doped catalysts exhibit a different behavior, the dispersion values obtained with the three different procedures being practically identical.

In Table 3 the chemisorption data of the catalysts reduced in hydrogen at 823 K (HTR) are reported. A significant decrease in oxygen and hydrogen chemisorption is

TABLE 3

Rh Dispersion in Catalysts Heated at 823 K in a Hydrogen Stream[a]

| Catalyst | D | |
|---|---|---|
| | $O_2$ | $H_2$ |
| $Rh/ZrO_2$ | 49 | 28 |
| $Rh/ZrO_2$-V | 60 | 47 |
| $Rh/ZrO_2/K$ | 61 | 24 |
| $Rh/ZrO_2/Y$ | 62 | 30 |
| $Rh/ZrO_2/P$[b] | 86(72) | 28 |

[a] For explanations, see Table 2.

[b] Number in parentheses is the value after correction for the oxygen chemisorbed by the support (see text).

observed, which formally implies a decrease in Rh dispersion. In this case, too, the Rh dispersion evaluated from oxygen chemisorption is greater than that evaluated from hydrogen chemisorption. If the HTR samples are treated with oxygen at 823 K and then re-reduced in a hydrogen stream at 523 K (LTR), following the procedure outlined under Experimental, the dispersion data become very similar to those reported in Table 2 for the LTR samples. These results show that the chemisorption properties of supported rhodium decrease on increasing the temperature of thermal treatments; this decrease is a reversible process.

### *FT-IR Photoacoustic Spectroscopy*

The FT-IR/PA spectrum of $Rh_4(CO)_{12}/ZrO_2$ (Fig. 1) shows bands at 2060 and 1819 $cm^{-1}$ assigned to CO linearly and bridge-bonded to $Rh^0$, respectively, and bands at 2092 and 2015 $cm^{-1}$ assigned to a geminal dicarbonyl complex on $Rh^I$. The band of bridging CO is much weaker and shifted to lower frequency compared to $Rh_4(CO)_{12}$ (*31, 32*), probably owing to the interaction of the CO ligand with $ZrO_2$ (*23*). The gem-dicarbonyl bands appear at lower frequency with respect to those occurring on an $Al_2O_3$ support (*33*), confirming the existence of an interaction, direct or indirect (via Rh), between the CO ligand and the support. These $ZrO_2$-promoted IR shifts are likely to mask any eventual IR effect of the doping agents present at very low concentration relative to Zr; in fact no appreciable frequency shift has been observed in the bands of the catalysts containing $K_2O$, $P_2O_5$, or $Y_2O_3$. These samples show the presence of CO linearly bonded to both $Rh^0$ and $Rh^I$ species together with a smaller amount of bridging CO revealed by a band centered at about 1820 $cm^{-1}$.

The supported carbonyls kept in the IR cell under He atmosphere at 305 K showed a slow change revealed by the growth of a band centered at 2349 $cm^{-1}$ due to $CO_2$ and by a gradual decrease in the bands of linear and bridging CO on $Rh^0$. At the same time, a group of weak and broad bands in the region 1700–1200 $cm^{-1}$, typical of various carbonate complexes, slightly increased in

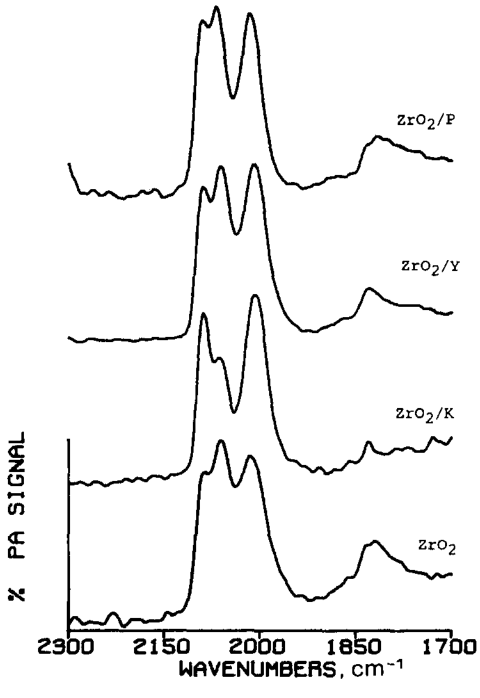

FIG. 1. FT-IR/photoacoustic spectra of $Rh_4(CO)_{12}$ on pure and doped $ZrO_2$.

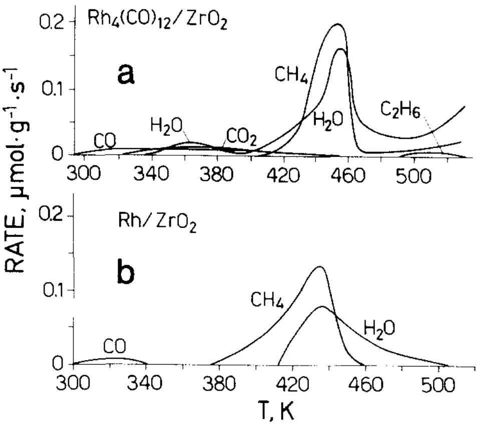

FIG. 2. Product formation rates from TPR in a $H_2$ flow on (a) $Rh_4(CO)_{12}/ZrO_2$ and (b) $Rh/ZrO_2$ after recarbonylation of the reduced sample.

intensity, whereas the broad band at about 3400 cm$^{-1}$, due to surface hydroxyls, did not show any appreciable change in intensity.

### *Temperature-Programmed Reduction*

A typical TPR profile in hydrogen is reported in Fig. 2. Carbon monoxide, carbon dioxide, methane, ethane, and water were detected in TPR measurements. TPR patterns of the freshly supported Rh carbonyl cluster and those of the recarbonylated samples show different shapes and temperatures for the individual peaks. In Table 4 the initial ($T_i$), final ($T_f$), and maximum peak ($T_m$) temperatures are reported for all the products observed with the various catalysts. In all cases the $T_m$ values for CO are lower for the recarbonylated samples than for the supported carbonyls, revealing that the metal carbon bond is weaker in the former than in the latter.

The most significant differences between pure and doped samples are (1) an increase in $T_m$ for all the products from $Rh/ZrO_2/K$, with the exception of a lower $T_m$ value for CO desorption from the supported carbonyl; and (2) the absence of a detectable amount of CO desorbed from recarbonylated $Rh/ZrO_2/Y$ and the low value for methane maximum peak temperature. Yttria seems to favor methane formation.

### *Temperature-Programmed Reaction in Flowing $H_2$–CO Mixture*

A 3/1 $H_2$/CO mixture was passed over the reduced samples following the same procedure as previously described for the hydrogen TPR runs. Typical plots of the rate of product formation as a function of temperature are reported in Fig. 3. Rates of formation of the most abundant products, methane and carbon dioxide, were analyzed by Arrhenius plots to evaluate the frequency factors and the apparent activation energies (Table 5).

TABLE 4

Characteristic Peak Temperatures from TPR of Supported Rh Catalysts[a]

| Catalyst | Peak temperature (K) | | | | | |
|---|---|---|---|---|---|---|
| | CO | | | $CO_2$ | | |
| | $T_i$ | $T_m$ | $T_f$ | $T_i$ | $T_m$ | $T_f$ |
| $Rh/ZrO_2$ (F)[b] | 300 | 340 | 450 | 320 | 360 | 450 |
| $Rh/ZrO_2$ (R) | 300 | 320 | 340 | — | — | — |
| $Rh/ZrO_2/K$ (F) | 325 | 370 | 465 | 430 | 460 | 480 |
| $Rh/ZrO_2/K$ (R) | 343 | 360 | 400 | — | — | — |
| $Rh/ZrO_2/Y$ (F) | 365 | 405 | 435 | 415 | 445 | 460 |
| $Rh/ZrO_2/Y$ (R) | — | — | — | — | — | — |
| $Rh/ZrO_2/P$ (F) | 315 | 395 | 425 | 405 | 420 | 425 |
| $Rh/ZrO_2/P$ (R) | 305 | 330 | 380 | — | — | — |
| | $CH_4$ | | | $H_2O$ | | |
| | $T_i$ | $T_m$ | $T_f$ | $T_i$ | $T_m$ | $T_f$ |
| $Rh/ZrO_2$ (F) | 400 | 450 | — | 340 | 450 | — |
| $Rh/ZrO_2$ (R) | 380 | 440 | 460 | 415 | 440 | 510 |
| $Rh/ZrO_2/K$ (F) | 420 | 465 | 525 | 450 | 465 | 515 |
| $Rh/ZrO_2/K$ (R) | 410 | 450 | 495 | 440 | 460 | 495 |
| $Rh/ZrO_2/Y$ (F) | 430 | 455 | 505 | 445 | 460 | >495 |
| $Rh/ZrO_2/Y$ (R) | 375 | 430 | 495 | 430 | 455 | >495 |
| $Rh/ZrO_2/P$ (F) | 415 | 445 | 495 | 435 | 455 | >475 |
| $Rh/ZrO_2/P$ (R) | 395 | 445 | 500 | 440 | 460 | >475 |

[a] $T_i$, $T_m$, and $T_f$ are the initial, maximum, and final peak temperatures.

[b] F, freshly prepared catalysts; R, recarbonylated after reduction at 523 K.

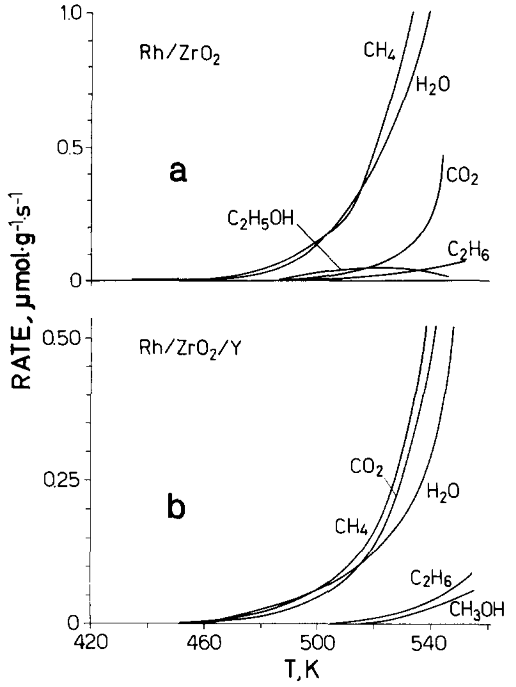

FIG. 3. Product formation rates from TPR on (a) $Rh/ZrO_2$ and (b) $Rh/ZrO_2/Y$ in a flow of 3 : 1 $H_2/CO$ mixture.

For carbon dioxide the apparent activation energy on all the catalysts is not significantly different, the average value being around 125 kJ/mole. The apparent activation energy for methane formation on $Rh/ZrO_2/K$ (160 kJ/mole) is significantly higher than the values of the other catalysts, which are in the range 110–115 kJ/mole. As to the frequency factors, for carbon dioxide no significant differences are observed on the various catalysts, taking into account the compensation effect due to the small variation in the activation energy. As for methane, the value observed on $Rh/ZrO_2/K$ is three orders of magnitude greater than that on the other catalysts.

These results show that all the catalysts behave similarly, except $Rh/ZrO_2/K$, for which methane formation is controlled by the high value of the activation energy, whose effect is not compensated by the increase in the frequency factor.

### *Catalytic Activity*

All catalysts were tested in the hydrogenation of CO under differential conditions at 493 K. Activity and selectivity (expressed as carbon efficiency) of bulk- and surface-doped catalysts activated in $H_2$ at 523 K were investigated first. As shown in Table 6, the P-doped catalyst displays slightly higher activity upon bulk doping; K-doped $Rh/ZrO_2$ has a lower activity for hydrocarbon formation and a significantly higher selectivity to ethanol, the trend being more evident on surface-doped than bulk-doped catalysts.

All surface-doped catalysts have been tested under the same reaction conditions used before to determine the influence of activation temperature (523 and 823 K). For comparison, the data are reported in Table 6. In the temperature range investigated, the activation temperature seems to have no influence on product distribution except for $Rh/ZrO_2/P$, for which the higher activation temperature results in a decrease in carbon chain growth and, most of all, an inversion of methanol and ethanol selectivities. As to conversion, a decrease after HTR (823 K) is generally evident, except for $Rh/ZrO_2/Y$.

The reactivities of the catalysts activated at 523 or 823 K, evaluated as turnover number (T.N.), by computing the surface Rh

TABLE 5

Frequency Factor *A* (mole/g · s) and Activation Energy *E* (kJ/mole) for Methane and Carbon Dioxide Formation from TPR Runs in a Flowing $H_2$–CO Mixture[a]

| | $CH_4$ | | $CO_2$ | |
|---|---|---|---|---|
| | *A* | *E* | *A* | *E* |
| $Rh/ZrO_2$ | $2 \times 10^5$ | 110 | $6 \times 10^4$ | 120 |
| $Rh/ZrO_2/K$ | $8 \times 10^8$ | 160 | $6.5 \times 10^5$ | 125 |
| $Rh/ZrO_2/Y$ | $3.5 \times 10^4$ | 110 | $2.3 \times 10^6$ | 130 |
| $Rh/ZrO_2/P$ | $2.5 \times 10^5$ | 115 | $4 \times 10^6$ | 135 |

[a] Heating rate = 2 K/min; GHSV = 1200.

TABLE 6

Activity of Surface-Treated and of Bulk-Doped (B) Rh Catalysts at 493 K as a Function of Activation Temperature[a]

| Catalyst | Activation temperature (K) | CO conversion (%) | Product distribution as carbon efficiency[b] | | | | | | |
|---|---|---|---|---|---|---|---|---|---|
| | | | $C_1$ | $C_2$ | $C_3$ | $C_4$–$C_7$ | MeOH | EtOH | $CH_3CHO$ |
| $Rh/ZrO_2$ | 523 | 3 | 58 | 6.7 | 9.6 | 7.2 | 3 | 14 | 0.5 |
| | 823 | 1.2 | 58 | 7.3 | 9.6 | 6.0 | 2.8 | 16 | 0.3 |
| $Rh/ZrO_2$(V) | 523 | 3.9 | 59 | 6.9 | 10 | 8.6 | 3.1 | 13 | 0.4 |
| | 823 | 3.2 | 59 | 6.5 | 10 | 7.2 | 1.8 | 15 | 0.5 |
| $Rh/ZrO_2/K$ | 523 | 2.1 | 49 | 9.2 | 7.0 | 2.2 | 3.3 | 28 | 1 |
| | 823 | 0.6 | 49 | 10 | 7.1 | 1.3 | 3.1 | 29 | 0.5 |
| $Rh/ZrO_2/K$(B) | 523 | 3.1 | 54 | 9.7 | 9.4 | 3 | 1.5 | 21.5 | 1 |
| $Rh/ZrO_2/Y$ | 523 | 3.3 | 60 | 6.4 | 11 | 7 | 2.5 | 13 | 0.3 |
| | 823 | 3.7 | 59 | 6.5 | 10 | 7.1 | 1.9 | 15 | 0.5 |
| $Rh/ZrO_2/Y$(B) | 523 | 3 | 60 | 8.4 | 12 | 7 | 2.6 | 10 | 0.1 |
| $Rh/ZrO_2/P$ | 523 | 2.7 | 59 | 7.6 | 10 | 6.6 | 4 | 13 | — |
| | 823 | 0.5 | 55 | 10 | 10 | 1.7 | 20 | 3.3 | — |
| $Rh/ZrO_2/P$(B) | 523 | 3.8 | 60 | 8.2 | 12 | 7.1 | 2.6 | 10 | 0.1 |

[a] $H_2/CO = 3/1$; GSHV = 1000; $P_{tot} = 0.1$ MPa.

[b] Carbon efficiency = $100(n_iA_i/\sum n_iA_i)$, where $n_i$ = carbon number of product $i$; $A_i$ = moles of product $i$.

sites on the basis of oxygen or of hydrogen chemisorption, are reported in Table 7. Differences in the two sets of values reveal that T.N. strongly depends on the method of evaluation of surface sites.

The influence of feed composition on product distribution is given in Table 8 for $H_2/CO$ ratios of 3/1 and 2/1. On all the catalysts, upon increasing the CO content in the feed, the conversion decreases, and the carbon efficiency for methane strongly decreases, whereas that for higher hydrocarbons increases. In all cases, the total carbon efficiency for hydrocarbons decreases whereas that for oxygenated compounds increases slightly. Due to the large decrease in the conversion, the productivities of the oxygenates on all the catalysts decrease on increasing CO partial pressure.

Because of the general interest in enhancing the selectivity to ethanol, we tried to obtain better insight into the promising $Rh/ZrO_2/K$ catalyst by varying the K content in the support. Catalysts containing 0.15 to 3% (w/w) K were prepared and tested under the usual conditions. Activity

TABLE 7

Effect of Activation Temperature on Turnover Number (T.N.)[a]

| Catalyst | Activation temperature (K) | T.N. × $10^4$ [(moles CO)/(s · g atom Rh)][b] | |
|---|---|---|---|
| | | *A* | *B* |
| $Rh/ZrO_2$ | 523 | 12 | 16 |
| | 823 | 2.5 | 16 |
| $Rh/ZrO_2$(V) | 523 | 15 | 16 |
| | 823 | 16 | 20 |
| $Rh/ZrO_2/K$ | 523 | 7 | 7.2 |
| | 823 | 3 | 7.4 |
| $Rh/ZrO_2/Y$ | 523 | 11 | 13 |
| | 823 | 18 | 36 |
| $Rh/ZrO_2/P$ | 523 | 9 | 13 |
| | 823 | 2 | 5.6 |

[a] Reaction conditions: $T = 493$ K; $H_2:CO = 3:1$; $P = 0.101$ MPa.

[b] (A) Rh sites evaluated from oxygen chemisorption. (B) Rh sites evaluated from hydrogen chemisorption.

TABLE 8

Effect of Feed Composition on Activity and Carbon Efficiency[a]

| Catalyst | $H_2/CO$ | Conversion | $C_1$ | $C_2$ | $C_3$ | $C_4$–$C_7$ | $CH_3OH$ | EtOH | $CH_3CHO$ | $C_2H_6CO$ |
|---|---|---|---|---|---|---|---|---|---|---|
| $Rh/ZrO_2$ | 3/1 | 3 | 59 | 7 | 9.5 | 7 | 3 | 14 | 0.5 | — |
| | 2/1 | 2 | 49 | 8 | 14 | 8.5 | 3.5 | 16 | 1 | — |
| $Rh/ZrO_2/K$ | 3/1 | 2.1 | 49 | 9 | 7 | 2.5 | 3.5 | 28 | 1 | — |
| | 2/1 | 1.3 | 39 | 10 | 8 | 3.5 | 4.5 | 34 | 1 | 0.2 |
| $Rh/ZrO_2/Y$ | 3/1 | 3.3 | 50 | 7 | 11 | 6 | 2 | 13 | 1 | — |
| | 2/1 | 2.2 | 49 | 7 | 15 | 8 | 3 | 18 | 0.5 | — |
| $Rh/ZrO_2/P$ | 3/1 | 2.7 | 59 | 8 | 10 | 6 | 4 | 13 | — | — |
| | 2/1 | 1 | 52 | 9 | 13 | 8 | 5 | 13 | — | — |

[a] $T = 493$ K; $P = 0.101$ MPa; GHSV = 1000.

and carbon efficiency data as a function of K concentration are shown in Fig. 4. The catalysts containing 3% K turned out to be totally inactive. CO conversion decreases monotonically with increasing K content, whereas selectivity to ethanol and oxygenates shows maximum (28 and 33%, respectively) around 0.3% (w/w) K: this value corresponds to a K/surface Rh ratio of 0.85.

## DISCUSSION

### *Chemisorption Measurements*

Oxygen chemisorption measurements are generally considered adequate for determination of the number of surface Rh atoms, as the oxidation stoichiometry is independent of particle size and of the support (*34*). In the case of hydrogen, however, chemisorption stoichiometry depends strongly on Rh particle size and on the metal–support interaction. Indeed, the H/Rh ratio may change from values greater than unity for small particles (*35–38*) to values lower than unity for larger particles (*16, 34, 39*), although no strict correlation exists between particle size and chemisorption stoichiometry. Hydrogen chemisorption is a good tool with which to reveal strong metal–support interactions (SMSI); a decrease in the hydrogen chemisorption properties of a metal has been attributed by some authors to a charge transfer between the support and the metal (*26*), although this is addressed further below.

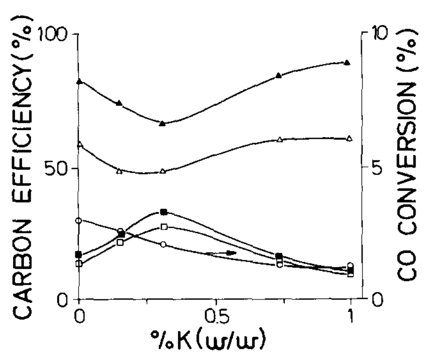

FIG. 4. CO conversion and carbon efficiency for Rh/$ZrO_2$/K catalyst as a function of K content (% w/w). Reaction conditions: 493 K; 0.1 MPa; GHSV 1000. ○, CO conversion; △, methane; ▲, hydrocarbons; □, ethanol; ■, oxygenates.

The chemisorption data reported in Tables 2 and 3 indicate a decrease in both chemisorbed hydrogen and chemisorbed oxygen after HTR, the former being greater. If a particle size increase were responsible for the decrease in oxygen chemisorption after HTR, a proportional decrease in chemisorbed hydrogen would result. The general indication of the chemisorption data seems to be the occurrence of SMSI. This is in general agreement with previous findings on Rh catalysts dispersed on commercial $ZrO_2$, for which a model involving both partial coverage of the metal particles by the support and a change in the electron density of the metal has been proposed to account for the experimental data (*40*). On the basis of this model we suggest that the decrease in oxygen chemisorption is due mainly to a masking effect of the rhodium particles, following a migration of $ZrO_2$ surface layers on metal particles with formation of $ZrO_2$ patches (*41*). The intensity of this phenomenon may depend on the mobility of zirconia surface layers, which in turn is correlated with the phase composition and with the presence of additives on the surface. The general indication arising from a comparison of LTR and HTR oxygen chemisorption seems to be that with the exception of P, the mobility of the surface layer of the doped and the tetragonal-rich support is only slightly lower than that of the regular monoclinic $ZrO_2$.

This and similar models, however, cannot be viewed simply as a way to impose stereochemical constraints that result in the masking of some chemisorption sites on the metal surface, since this would not account for the differences in $O_2$ and $H_2$ chemisorption data especially after low-temperature reduction. A useful parameter to analyze the chemisorption data is the ratio ($R$) of the dispersions calculated from $H_2$ and $O_2$ chemisorption after either low- or high-temperature reduction (Table 9). By assuming that $O_2$ is able to titrate all of the metal sites actually exposed (*34*), we suggest that the value of $R$ be viewed as indicative of the metal "affinity" toward $H_2$. As shown in Table 9 all the catalysts have $R$ values (which we ascribe to hydrogen "affinities") well below unity, with the exception of $Rh/ZrO_2(V)$ and $Rh/ZrO_2/K$. Moreover, no apparent difference between surface- and bulk-doped catalysts results after treatments at 523 K. The $R$ values decrease after HTR, particularly for the doped catalysts.

TABLE 9

Ratio ($R$) between the Dispersion Calculated from Hydrogen and from Oxygen Chemisorption on Catalysts Activated at 523 or 823 K

| | $R$ | | |
|---|---|---|---|
| | 523 K | 823 K | 523 K/823 K |
| $Rh/ZrO_2$ | 0.77 | 0.57 | 1.4 |
| $Rh/ZrO_2/V$ | 0.91 | 0.78 | 1.2 |
| $Rh/ZrO_2/K$ | 0.98 | 0.4 | 2.5 |
| $Rh/ZrO_2/K$ (B) | 0.94 | | |
| $Rh/ZrO_2/Y$ | 0.83 | 0.5 | 1.7 |
| $Rh/ZrO_2/Y$ (B) | 0.84 | | |
| $Rh/ZrO_2/P$ | 0.69 | 0.32 | 2.1 |
| $Rh/ZrO_2/P$ (B) | 0.72 | | |

To account for these observations, we suggest that even after low-temperature reduction, pure $ZrO_2$, behaving as a Lewis acid, exerts an effect on the metal particle which results in a partial positive charge, which in turn decreases its hydrogen "affinity." This view seems adequate to justify the drop in hydrogen "affinity" after HTR treatment, on the basis of the models suggested for SMSI. Moreover, it can explain the higher values found for the K-doped supports, at least after LTR, for which a partial neutralization of acidity has been already suggested by other authors. As for $Rh/ZrO_2(V)$, the most apparent difference from the other samples seems to be the phase composition of the support; however, no correlation could be found in the literature between phase composition and surface acidity in the case of $ZrO_2$. Further discussion of the $O_2$ chemisorption properties of the P-doped sample is needed. At variance with the other catalysts, $Rh/ZrO_2/P$ shows little difference in $O_2$ chemisorption after HTR (Tables 2 and 3). We have seen that after HTR, the support itself adsorbs a certain amount of gas; this is most likely due to reoxidation of P oxides of lower oxidation states (probably $P_4O_6$) formed by reduction with $H_2$ at 823 K, because of the modest redox potential of the $P_4O_{10}/P_4O_6$ couple. The corrected chemisorption values (in parentheses in Table 3) are in line with the other data.

The variation in $R$ (hydrogen "affinity") for the various catalysts and with temperature cannot be explained in terms of a masking effect of Rh particles. Therefore one has to assume that patch formation is coupled with transfer of a positive charge on Rh atoms that causes a decrease in hydrogen "affinity." The question is how this charge transfer may occur. Should $Zr^{3+}$ species be present, even though $ZrO_2$ is very stable and difficult to reduce, electron transfer from the reduced Zr ions to Rh atoms must occur, with formation of a partially ionic bond and increase in hydrogen affinity (*42*). Electron transfer from rhodium to the support, as in a metal–semiconductor junction, would give rise to a so-called image potential that would suppress the further transfer of electrons (*41, 43*), thus making it difficult to explain how the resulting small transfer of electrons could cause the observed and not negligible change in the chemical behavior of the Rh particles. To account for our hydrogen affinity data, we suggest that owing to the high dispersion of rhodium, the phenomena at the metal–support borderline must be regarded carefully, mainly when relevant decoration effects are present. This means that rhodium at the borderline may interact with acid sites of zirconia (*44, 45*) with the formation of partially oxidized $Rh^I$ species that have low affinity for hydrogen chemisorption. Simple calculations show that it is sufficient to decorate 30% of the metal surface by means of three or four $ZrO_2$ patches, to halve the hydrogen chemisorption on Rh particles with a diameter of 2 nm. The possibility that rhodium gives oxidized $Rh^I$ species may be related to the low value of the first ionization potential.

The ability of $ZrO_2$ acidic sites to react with rhodium depends on the surface composition. Figure 4 shows that, at 523 K, $K_2O$ lowers the number or reactivity of acidic surface sites as the hydrogen affinity increases, whereas $P_2O_5$ increases their number or reactivity as the hydrogen affinity decreases. The behavior of the other catalysts is intermediate.

After HTR treatment the *R* values of all the catalysts are quite similar; a general decrease in hydrogen chemisorption is observed, except for $Rh/ZrO_2(V)$, probably owing to the stability of the subcooled tetragonal phase. This decrease in hydrogen "affinity" may be explained by a general increase in $ZrO_2$ surface acidity independent of the doping agent. It has been shown (*45*) that the acidity of surface hydroxyl groups on $ZrO_2$ increases on heating to 673 K.

### *Infrared Spectroscopic Analysis*

The results from IR analysis can be summarized as follows:

1. Doping of $ZrO_2$ with $K_2O$, $P_2O_5$, and $Y_2O_3$ causes no significant frequency shift in the IR bands of $Rh_4(CO)_{12}/ZrO_2$.
2. Supported Rh carbonyl is unstable under IR irradiation and decomposes with the formation of carbon dioxide.
3. The concentration of $ZrO_2$ surface hydroxyls does not change appreciably during cluster decomposition.

The IR data accordingly suggest that, at low temperature, carbon dioxide formation takes place through the Boudouard reaction and that no water-gas shift reaction or surface hydroxyl reaction occurs. Rh carbonyl decomposition involves the disappearance of linear and bridged carbonyls bonded to $Rh^0$ and leaves $Rh^I(CO)_2$ as the predominant surface species.

### *TPR Results*

The supported rhodium carbonyls and the recarbonylated samples react under TPR conditions according to the following scheme:

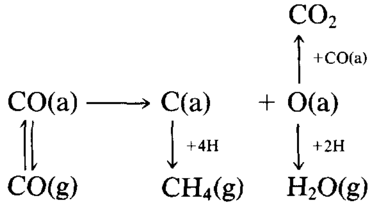

The two main reactions of adsorbed CO are desorption and dissociation to carbon and oxygen; these latter species may react with hydrogen to give methane and water, respectively, and oxygen may react with carbon monoxide to give carbon dioxide. The difference in reactivity between the supported carbonyls and the recarbonylated samples, revealed by TPR results, reflects the different surface structures of the two set of samples.

A previous study showed that the CO/Rh ratio is lower in recarbonylated $Rh/ZrO_2$ samples than in the supported carbonyls (*46*). Actually, it is generally accepted that the chemisorption of CO on supported rhodium induces the disruption of metal crystallites and the formation of $Rh^I(CO)_2$ species (*32, 47, 48*).

$T_i$ or $T_m$ values for CO desorption are indicative of metal–carbonyl bond strength. Comparison of the values for supported carbonyls and recarbonylated samples shows that all characteristic temperatures are significantly lower in the latter case. This fact allows the following two conclusions to be drawn: (1) the recarbonylation process does not lead to formation of the initial carbonyl cluster; (2) the CO–Rh bond energy of recarbonylated samples is lower than in the supported carbonyl clusters (*49*).

$CO_2$ is formed only on the supported carbonyls and its peak temperature is lower than that of $CH_4$. The mechanism of formation via CO disproportionation is suggested by IR and TPD results (*32*) and is in agreement with a widely accepted scheme (*20*). The stronger CO–Rh bond in the supported carbonyls implies an easier CO dissociation; subsequent CO oxidation and $CO_2$ evolution occur until a sufficient number of free active sites are available for hydrogen adsorption and the following hydrogenation reaction.

The lower CO/Rh value in the recarbonylated samples may be indicative of a coordinative unsaturation of rhodium and of the presence of free sites available for hydrogen chemisorption; under these conditions $CH_4$ rather than $CO_2$ is formed initially during TPR, with peak maxima at lower temperature compared with the carbonyl clusters. The $T_m$ value of methane is higher on $Rh/ZrO_2/K_2O$, both in supported carbonyls and in recarbonylated samples: $K_2O$ lowers rhodium activity in either CO dissociation or hydrogenation reactions.

For all samples water and methane have the same $T_m$ values, showing that their formation has a common rate-determining step identified in the dissociation of adsorbed CO, whereas hydrogenation of carbon and oxygen atoms is a fast process when active sites are available for hydrogen adsorption.

In TPR runs, hydrogen flows through the sample the surface of which has been previously saturated with carbon monoxide. In the TPR–$H_2$/CO case, a stream of hydrogen and carbon monoxide flows through the catalytic bed at constant partial pressure, so that both reagents are adsorbed and their surface concentration is determined by the temperature of the system. The higher values of $T_i$ for $CH_4$ in TPR–$H_2$/CO runs indicate that in this case the rate of formation is inhibited by CO chemisorption.

TPR runs in a flowing $H_2$/CO mixture, i.e., under conditions closer to those of catalytic activity measurements than standard TPR, indicate that all catalysts have similar hydrogenation properties except $Rh/ZrO_2/K$, on which the rate of methane formation is significantly lower. This conclusion is in agreement with the results of standard TPR runs.

### *Catalytic Properties*

A comparison of the catalytic properties of the various samples can be made on the basis of their specific activity as defined by the turnover number.

Two measurements of surface Rh sites have been performed, namely by oxygen and by hydrogen chemisorption, and the relevant T.N.'s are reported in Table 7. The respective sets of T.N.'s have different values, but whereas the same trend is evident for the LTR (523 K) catalysts, the HTR (823 K) catalysts exhibit a completely different behavior. In fact, upon increasing the reduction temperature, the T.N. evaluated from oxygen chemisorption increases on Rh/$ZrO_2$/Y; it does not change on Rh/$ZrO_2$(V), and it decreases on all the other catalysts, by a factor of about 2 on Rh/$ZrO_2$/K, about 4 on Rh/$ZrO_2$/P, and about 5 on Rh/$ZrO_2$. These data suggest that the number of Rh sites determined by oxygen chemisorption is not representative of the sites active in the reaction.

As for the T.N.'s from hydrogen chemisorption, the values are virtually the same after LTR and HTR for Rh/$ZrO_2$, Rh/$ZrO_2$(V), and Rh/$ZrO_2$/K. This seems to indicate that the nature of the active sites does not change by thermal treatments, which simply affect their number as shown by chemisorption data, the activity of the surface sites remaining the same. The hydrogen-scaled T.N. on Rh/$ZrO_2$/Y and Rh/$ZrO_2$/P changes after HTR: it increases three times on the former catalyst and is halved on the latter. $P_2O_5$ doping increases the surface acidity of $ZrO_2$, and as has been previously suggested, favors the formation of $Rh^I$ and decreases the hydrogen affinity of rhodium. However, this effect is already computed in calculating the T.N. Most probably the HTR treatment favors the mobility of $P_2O_5$, the concentration of which is increased at the borderline between metal and support, with a consequent increase in acidity which may explain the observed decrease in T.N. upon HTR. We suggest that, under reaction conditions, this results in a lower capacity to chemisorb hydrogen which is balanced by an increase in CO chemisorption, the effect of which is to "poison" the surface and decrease the rate of the reaction.

An alternative, or complementary view, leading to the same conclusion, may involve "poisoning" of the surface by coordinative interaction from $P_4O_6$ produced *in situ* after HTR as previously described. In this respect the effect of $P^{III}$ donors on Rh metal catalysts in hydrogenation reactions has been reported elsewhere (*50–52*). As for the T.N. enhancements by $Y_2O_3$, some authors have shown that the activity and sometimes the selectivity of supported Rh, Pd, and Pt can be enhanced by rare earth oxides ($La_2O_3$, $Nd_2O_3$, $CeO_2$, etc.) (*21, 53–55*) and by the so-called "oxophilic oxides," i.e., oxides that can easily give redox reactions (*56–59*). It has recently been reported (*60*) that titania deposited over polycrystalline rhodium foil increases CO hydrogenation and a maximum in activity has been found for a coverage of 0.15 of a monolayer. The increase in activity has been attributed to the formation, under reaction conditions, of $Ti^{3+}$ species that participate at the metal oxide borderline in the CO dissociation step.

A growing body of work suggests that the activity enhancement of supported rhodium by promoter oxides can be ascribed to the migration of reduced oxides onto the surface of the supported metal particles. Therefore, we infer that the enhancement of Rh/$ZrO_2$/Y T.N. after HTR may be attributed to the formation of reduced $Y_2O_x$ at the borderline between oxide patches and metal particles.

As far as selectivity is concerned, Rh/$ZrO_2$, Rh/$ZrO_2$(V), and Rh/$ZrO_2$/Y have practically the same carbon efficiencies, which do not change with LTR or HTR treatment. The different phase compositions of Rh/$ZrO_2$ and Rh/$ZrO_2$(V) do not appear to influence the T.N. and selectivity of the catalysts. The effect of $Y_2O_3$ is somewhat surprising since the increase in T.N. after HTR is not paralleled by any variation in selectivity. According to the previously assumed model, the role of $Y_2O_3$ is to favor CO dissociation, which is generally considered the rate-determining step in CO + $H_2$ reactions. However, so as not to change the carbon efficiencies we must assume that the rates of formation of the individual products from the adsorbed CO and $H_2$ species increase to the same extent in the HTR catalyst.

The values for carbon efficiency and their variation with temperature for Rh/$ZrO_2$/K and Rh/ZrO$_2$/P are different from those previously discussed and require a different analysis.

All the K-doped catalysts investigated in this study have a high selectivity toward C$_2$ and oxygenated compounds which does not change after HTR treatment, whereas the CO conversion decreases and the T.N. remains unchanged. The effect of alkali metals on the activity and selectivity of group VIII metals is equivocal, as experimental data with opposite results and conclusions have been reported. Alkali salts decrease the activity of Ni supported on SiO$_2$ in the CO hydrogenation reaction, but increase it when Ni is supported on SiO$_2$–Al$_2$O$_3$ (*61*). The catalyst reduction or activation temperatures modify the effect of alkali metal: Pd/SiO$_2$ doped with different alkalis changes its adsorption properties and its reactivity with the reduction temperature, mainly because of the variation in CO adsorption states (*62*). Alkalis decrease the dissociation of CO chemisorbed on Pd, because they promote linear-bonded CO. In any case the unpromoted Pd/SiO$_2$ catalysts are more active than the alkali-promoted catalysts.

The decrease in the catalytic activity and the increase in hydrogen chemisorption can be attributed either to an increase in ZrO$_2$ surface mobility, which favors the formation of patches on Rh particles, or to a disruption of Rh metal particles. In both cases smaller Rh ensembles are formed. On the catalyst surface thus modified, chemisorption of pure hydrogen is favored, but under the reaction conditions, the competitive chemisorption of carbon monoxide inhibits that of hydrogen, and hence the hydrogenation of CO is lowered.

The activity of the Rh/ZrO$_2$/K catalyst decreases strongly on increasing the content of K$_2$O, and is completely suppressed at 493 K for 3% (w/w) K. It is not easy to explain such a strong variation only on the hypothesis of the increase in linearly bonded CO. Probably other phenomena take place by increasing the amount of K$_2$O, as for instance a decrease in the hydrogenation activity and/or an increase in the Boudouard reaction with formation of nonreacting adsorbed carbon (*62*).

The selectivity toward C$_2$ oxygenates of K-doped catalysts may be explained by an increase in linearly-bonded CO and the consequent decrease in the rate of formation of CH$_x$ species. This leads to a relative increase in the probability of their reaction with adsorbed CO rather than with adsorbed hydrogen. This view is supported by the observation that the maximum selectivity to ethanol corresponds to the minimum selectivity to methane (Fig. 4).

The most interesting results concerning the Rh/ZrO$_2$/P sample are the decrease in T.N. after HTR treatment and the joint inversion in selectivity to oxygenated compounds (Table 7). The latter consideration is consistent with the previously reported acidity arguments. We suggest that the effect of surface acidity is to stabilize isolated Rh species (probably as Rh$^{\mathrm{I}}$) on which both CO dissociation and hydrogen activation are unfavored, with a consequent increase in methanol formation in the reaction mixture. The same conclusion can be drawn on the basis of the interaction between P$^{\mathrm{III}}$ centers and the metal surface, which would result in a decrease in the average size of the Rh ensembles required for CO dissociation and chain growth.

Conversion and the carbon efficiency data for H$_2$/CO = 2 can be interpreted according to the previous discussion. By decreasing the H$_2$/CO ratio in the reacting mixture, CO adsorption is favored and hydrogen adsorption is inhibited. As a consequence, the hydrogenation reaction rate decreases and the surface CH$_x$ species statistically have a greater opportunity to react with adsorbed CO, with formation of oxygenated compounds. This explains the decrease in catalyst activities, due mainly to the decrease in the formation of hydrocarbons.

From the overall analysis of the reported data it can be concluded that the main effects of the investigated doping agents on Rh/$ZrO_2$ are (i) modification of the surface density of acidic and basic sites, and, as a consequence, of the $Rh^I$ sites localized near the borderlines of the patches or isolated species; and (ii) variation of the mobility of the surface layers of $ZrO_2$, which, by affecting the formation of patches over Rh particles, and therefore the number of sites at the borderlines between Rh and $ZrO_2$ patches, enhances the influence of the support on the activity and the selectivity of the catalyst.

## ACKNOWLEDGMENTS

The authors thank the Ministero della Pubblica Istruzione and the CNR-Progetto Finalizzato Energetica for financial support.

## REFERENCES

1. Bart, J. C. J., and Sneeden, R. P. A., *Catal. Today* **2,** 1 (1987).
2. Smith, K. J., and Anderson, R. B., *J. Catal.* **85,** 428 (1984). See also Natta, G., Colombo, U., Pasquon, I., *in* "Catalysis" (P. H. Emmett, Ed.), Vol. 5, p. 131. Reinhold, New York, 1957.
3. Poutsma, M. L., Elek, L. F., Ibarbia, P. A., Risch, A. P., and Rabo, J. A., *J. Catal.* **52,** 15 (1978).
4. Vannice, M. A., *Catal. Rev.-Sci. Eng.* **14,** 153 (1976).
5. Razzaghi, A., Hindermann, J. P., and Kienemann, A., *Appl. Catal.* **13,** 193 (1984).
6. Pijolat, M., and Perrichon, V., *Appl. Catal.* **13,** 321 (1985).
7. Bossi, A., Garbassi, F., Petrini, G., and Zanderighi, L., *J. Chem. Soc. Faraday Trans. 1* **78,** 1029 (1982).
8. Inoue, M., Miyake, T., Takegami, Y., and Inui, T., *Appl. Catal.* **11,** 103 (1984).
9. Takeuchi, K., Matsuzaki, T., Arakawa, H., and Sugi, Y., *Appl. Catal.* **18,** 325 (1985).
10. Fujimoto, K., and Oba, T., *Appl. Catal.* **13,** 289 (1985).
11. Ichikawa, M., *Bull. Chem. Soc. Japan* **51,** 2273 (1978).
12. Likholobov, V. A., Mayer, L. I., Bulgakov, N. N., Fedetov, A. V., and Steingauer, L. G., *in* "Homogeneous and Heterogeneous Catalysis" (Yu. Yermakov, and V. Likholobov, Eds.), p. 229. VNU Science Press, Utrecht, 1986.
13. Watson, P. R., and Somorjai, G. A., *J. Catal.* **72,** 347 (1981).
14. Watson, P. R., and Somorjai, G. A., *J. Catal.* **74,** 282 (1982).
15. Driessen, J. M., Poels, E. K., Hindermann, J. P., and Ponec, V., *J. Catal.* **82,** 26 (1983).
16. Katzer, J. R., Sleight, A. W., Gajardo, P., Michel, J. B., Gleason, E. F., and McMillan, S., *Faraday Discuss. Chem. Soc.* **72,** 121 (1981).
17. Solymosi, F., Tombacz, I., and Kocsis, M., *J. Catal.* **75,** 78 (1982).
18. Ichikawa, M., *in* "Homogeneous and Heterogeneous Catalysis" (Yu. Yermakov and V. Likholobov, Eds.), p. 819. VNU Science Press, Utrecht.
19. Knözinger, H., *in* "Homogeneous and Heterogeneous Catalysis" (Yu. Yermakov and V. Likholobov, Eds.), p. 789. VNU Science Press, Utrecht.
20. Sachtler, W. M. H., and Ichikawa, M., *J. Phys. Chem.* **90,** 4752 (1986).
21. Ichikawa, M., *Chemtech* **12,** 674 (1982).
22. Correa, F., Nakamura, R., Stimson, R. E., Burwell, R. L., and Shriver, D. F., *J. Amer. Chem. Soc.* **102,** 5112 (1980).
23. Ichikawa, M., and Fukushima, T., *J. Phys. Chem.* **89,** 1564 (1985).
24. Kikuzono, Y., Kagami, S., Naito, S., Onishi, T., and Tamaru, K., *Faraday Discuss. Chem. Soc.* **72,** 135 (1981).
25. Ichikawa, M., Fukushima, T., Yokoyama, T., Kosugi, N., and Kuroda, H., *J. Phys. Chem.* **90,** 1222 (1986).
26. Tauster, S. J., Fung, S. C., and Garten, R. L., *J. Amer. Chem. Soc.* **100,** 170 (1978).
27. Gu, G. S., *Acta Phys. Chim. Sin.* **1,** 177 (1985).
28. Benedetti, A., Fagherazzi, G., and Pinna, F., *J. Amer. Ceram. Soc.* **73,** 467 (1989).
29. Enzo, S., Fagherazzi, G., Benedetti, A., and Polizzi, S., *J. Appl. Crystallogr.* **21,** 536 (1988).
30. Toraya, H., Yoshimura, M., and Somiya, S., *J. Amer. Ceram. Soc.* **67,** 241 (1948).
31. Chini, P., and Martinengo, S., *Inorg. Chim. Acta* **3,** 315 (1969).
32. Zerlia, T., Carimati, A., Marengo, S., Martinengo, S., and Zanderighi, L., *in* "Structure and Reactivity of Surfaces" (C. Morterra, A. Zecchina, and G. Costa, Eds.), p. 943. Elsevier, Amsterdam, 1989.
33. Hamadeh, I. M., and Griffiths, P. R., *Appl. Spectrosc.* **41,** 682 (1987).
34. Yao, H. C., Japar, S., and Shelef, M., *J. Catal.* **50,** 407 (1977).
35. Vis, J. C., van't Blik, H. F. J., Huizinga, T., van Grondelle, J., and Prins, R., *J. Catal.* **95,** 333 (1985).
36. Vis, J. C., van't Blik, H. F. J., Huizinga, T., van Grondelle, J., and Prins, R., *J. Mol. Catal.* **25,** 367 (1984).
37. Kip, B. J., Duivenvoorden, F. B. M., Koningsberger, D. C., and Prins, R., *J. Catal.* **105,** 26 (1987).
38. Behm, R. J., Christmann, K., Ertl, G., Penta, V., and Schwankner, R., *in* "The Structure of Surfaces" (M. A. van Hove, and S. Y. Tong, Eds.), p. 257. Springer-Verlag, Berlin, 1985.

39. Underwood, R. P., and Bell, A. T., *J. Catal.* **109,** 61 (1988).
40. Dall'Agnol, C., Gervasini, A., Morazzoni, F., Pinna, F., Strukul, G., and Zanderighi, L., *J. Catal.* **96,** 106 (1985).
41. van der Lee, G., Bastein, A. G. T. M., van der Boogert, J., Schuller, B., Luo, H., and Ponec, V., *J. Chem. Soc. Faraday Trans. 1* **83,** 2103 (1986).
42. Sadeghi, H. R., and Henrich, V. E., *J. Catal.* **109,** 1 (1988).
43. Dalla Betta, R. A., and Boudart, M., *in* "Proceedings, 5th International Congress on Catalysis" (J. W. Hightower, Ed.), p. 1329. North Holland/American Elsevier, Amsterdam/New York, 1973.
44. Yamaguchi, T., Nakano, Y., and Tanabe, K., *Bull. Chem. Soc. Japan* **51,** 2482 (1978).
45. Nakano, Y., Iizuka, T., Hattori, H., and Tanabe, K., *J. Catal.* **57,** 1 (1979).
46. Carimati, A., Girelli, A., Marengo, S., Martinengo, S., Zanderighi, L., and Zerlia, T., *in* "Proceedings, 9th International Congress on Catalysis" (M. J. Phillips, and M. Ternan, Eds.), Vol. 2, p. 706. Chemical Institute of Canada, Ottawa, 1988.
47. Yates, J. T., Jr., Duncan, T. M., and Vaughan, R. W., *J. Chem. Phys.* **71,** 3908 (1979).
48. Van't Blik, H. F. J., Van Zon, J. B. A. D., Huizinga, T., Vis, J. C., Koningsberger, D. C., and Prins, R., *J. Phys. Chem.* **87,** 2264 (1983).
49. McKee, M. L., and Worley, S. D., *J. Phys. Chem.* **92,** 3699 (1988).
50. Cocco, G., Enzo, S., Pinna, F., and Strukul, G., *J. Catal.* **82,** 160 (1983).
51. Pinna, F., Gonizzi, G., Strukul, G., Cocco, G., and Enzo, S., *J. Catal.* **82,** 171 (1983).
52. Beringhelli, T., Gervasini, A., Morazzoni, F., Pinna, F., and Strukul, G., *J. Catal.* **88,** 3132 (1984).
53. Rieck, J. S., and Bell, A. T., *J. Catal.* **99,** 278 (1986).
54. Hindermann, J. P., Kiennemann, A., and Tazkritt, S., *in* "Structure and Reactivity of Surfaces" (C. Morterra, A. Zecchina, and G. Costa, Eds.), p. 481. Elsevier, Amsterdam, 1989.
55. Underwood, R. P., and Bell, A. T., *Appl. Catal.* **21,** 157 (1966).
56. Vannice, M. A., and Sudhakar, C., *J. Phys. Chem.* **88,** 2429 (1984).
57. Sachtler, W. M. H., Shriver, D. F., Hollenberg, W. B., and Long, A. F., *J. Catal.* **92,** 492 (1985).
58. Hicks, R. F., and Bell, A. T., *J. Catal.* **90,** 205 (1984).
59. van der Berg, F. G. A., Glezer, J. N. E., and Sachtler, W. M. H., *J. Catal.* **93,** 340 (1985).
60. Levin, M. E., Salmeron, M., Bell, A. T., and Somorjai, G. A., *J. Catal.* **106,** 401 (1987).
61. Chai, G-Y., and Falconer, J. L., *J. Catal.* **93,** 152 (1985).
62. Rieck, J. S., and Bell, A. T., *J. Catal.* **100,** 305 (1986).